Design of a Novel Servo-motorized Laser Device for Visual Pathways Diseases Therapy

Carlos Ignacio Sarmiento
Department of Hospital Bioengineering, National Institute of Neurology and Neurosurgery "Manuel Velasco Suárez", Mexico City, Mexico
carlos.sarmiento@itcm.edu.mx

V. B. Surya Prasath
Computational Imaging and VisAnalysis (CIVA) Lab Department of Computer Science University of Missouri-Columbia, Columbia MO 61211 USA
prasaths@missouri.edu

Abstract

We discuss a novel servo-motorized laser device and a research protocol for visual pathways diseases therapies. The proposed servo-mechanized laser device can be used for potential rehabilitation of patients with hemianopia, quadrantanopia, scotoma and some types of cortical damages. The device uses a semi spherical structure where the visual stimulus will be shown inside, according to a previous stimuli therapy designed by an ophthalmologist or neurologist. The device uses a pair of servomotors (with torque=1.5kg), which controls the laser stimuli position for the internal therapy and another pair for external therapy. Using electronic tools such as microcontrollers along with miscellaneous electronic materials, combined with LabVIEW based interface, a control mechanism is developed for the new device. The proposed device is well suited to run various visual stimuli therapies. We outline the major design principles including the physical dimensions, laser device's kinematical analysis and the corresponding software development.

Keywords: diseases therapy; neuroplasticity; biosensors; visual therapies; servomotor; Laser device

1. Introduction

Lesions occurred in front of the optical chiasm can cause visual field lose in only one eye whereas lesions behind can cause visual field lose in both eyes, more or less congruent to each other. The total destruction of any of the visual structures behind the optical chiasm in only one side causes contrateral homonymous hemianopia (Garoutte, 1981). Hemianopia, as with other visual field defects, is a result of retrochiasmatic lesions of visual pathways, produced by different causes, predominantly by vascular malfunctions (Lane *et al*., 2008).

There are two major techniques exist to enhance and/or repair visual field homonymous defects. The first one is to teach the patient to explore his or her blind side by compensatory saccadic movements and the other is to enhance the visual field by using a computer program to stimulate the border between the visible and damaged visual side (Schreiber *et al*., 2006). The scanning with ocular movements has been reported as an efficient tactic by the previous studies, reporting visual field enlargement up to 35° (Koons *et al*., 2010).

There are also related studies, which explore the different kinds of visual stimulus in waveform and frequency for therapies. In (Weiskrantz *et al*., 1991) the authors conclude, after a comparison of different forms, that a square wave form at approximately 3.7Hz can easily be seen by patients with visual dysfunctions. There is strong evidence supporting the effectiveness of the border zone stimulation and a possible activation of the extra-striate pathways (Romano, 2009; Marshall *et al*., 2008). Neuroplasticity is reported as a possible cause of this particular therapy method in humans with delicate behavior measurement, as measured by functional magnetic resonance (fMRI) images and positron emission tomography (PET). It has been observed that reactivation in some areas at the occipital lobe (Henriksson *et al*., 2007) and also activation in concentration areas (Romano, 2009).

It has been proved that the nervous system is continuously remodeled by experience and learning in response to an activity (Pascual-Leone *et al*., 2011). Moreover, it is observed that such remodeling mechanisms grow as the axon and dendrites reestablish new synaptic connections. Clinical practice and research have shown the possibility of total or partial restitution of the lost functions observing restoration of the affected visual functions. In this paper, we detail a novel servo-mechanized laser device, which can be used for such visual stimuli therapies.

The rest of the paper is organized as follows. Section 2 outlines the design of the proposed device and sensor, and Section 3 details the associated control mechanism that can help ophthalmologists and neurologists in using the device for various therapies. Section 4 concludes the paper.

2. Design of the Device

2.1. Physical Design

The device consists mainly of an acrylic semi-spherical structure (Figure 1(a)) where visual stimuli will be shown, according to a pre-designed therapy. Four servomotors will drive the lasers, two inside the structure (short distances drive the lasers, two inside the structure (short distance therapies) and two outside (middle-long distance therapies). A chin-rest must be used to have a better line of sight fixation. A webcam with infrared light will catch the Purkinje-Sanson images to identify the sight line (Borah, 2006; Halswanter, 2011; Pambakian *et al*., 2000). LabVIEW software is used to control the device, including an audio stimulus along with an image-processing pipeline. Finally a microcontroller is used to control the servo movements, laser beams and buzzers.

(a)

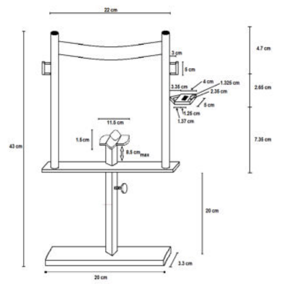

(b)

Figure 1. (a) Part of the acrylic structure where the patient is enclosed to avoid external stimulus; (b) Chin rest, corresponding proportions and measurements.

The semi-spherical structure must enclose the patient inside to avoid non-desired external stimulus. The device is attached to a servo-support structure, which contains the servo-mechanized stimulator for middle-to-long range distance therapies. The design of the chin-rest was based on classical techniques, dating back to Leonardo Da Vinci's manuscripts, which is designed according to the proportions of an average face. We use the face average measures for Mexican population (Panero and Zelnik, 1996), to design the chin-rest (Figure 1(b)). The laser servo driver is attached in the small square.

2.2. Laser Driver's Inverse and Direct Kinematics

Denavit-Hartenberg (DH) method was used for direct kinematic analysis (Fu *et al*., 1987). According to the definitions of variables and constants the DH parameters are given by:

i	θ	α	d	A
1	θ_1	90	d_1	0
2	θ_2	0	d_2	0

The homogeneous transformation matrix must be completed with DH parameters (Spong *et al.*, 2005) which is given as follows,

$$T = \begin{bmatrix} C\theta_1 C\theta_2 & -C\theta_1 S\theta_2 & S\theta_1 & d_2 S\theta_1 \\ S\theta_1 C\theta_2 & -S\alpha_1 S\theta_2 & -C\theta_1 & -d_2 C\theta_1 \\ S\theta_2 & C\theta_2 & 0 & d_1 \\ 0 & 0 & 0 & 1 \end{bmatrix} \qquad (1)$$

where C = Cosine; S = Sine. The inverse kinematics analysis was obtained using the geometrical method, which is shown in Figure 2(a).

The angle equations were obtained studying the model:

$$q_2 = \sin^{-1}\left[(P_{z_0} - l_1)/l_2\right] \qquad (2)$$

$$q_1 = \tan^{-1}\left(P_{y_0}/P_{x_0}\right). \qquad (3)$$

As the servo-driver will be attached in the chin-rest in a non-central area with respect to the semispherical structure shown in Figure 1(a), it is necessary to calculate a lag angle, according to the measurements from the chin-rest, see Figure 2(b). This was done using a hybrid formula based on the law of cosines,

$$B = \cos^{-1}\left(\frac{c - b\cos(A)}{\sqrt{b^2 + c^2 - 2bc}}\right). \qquad (4)$$

We next describe the control mechanism for the laser device along with the software modules used here.

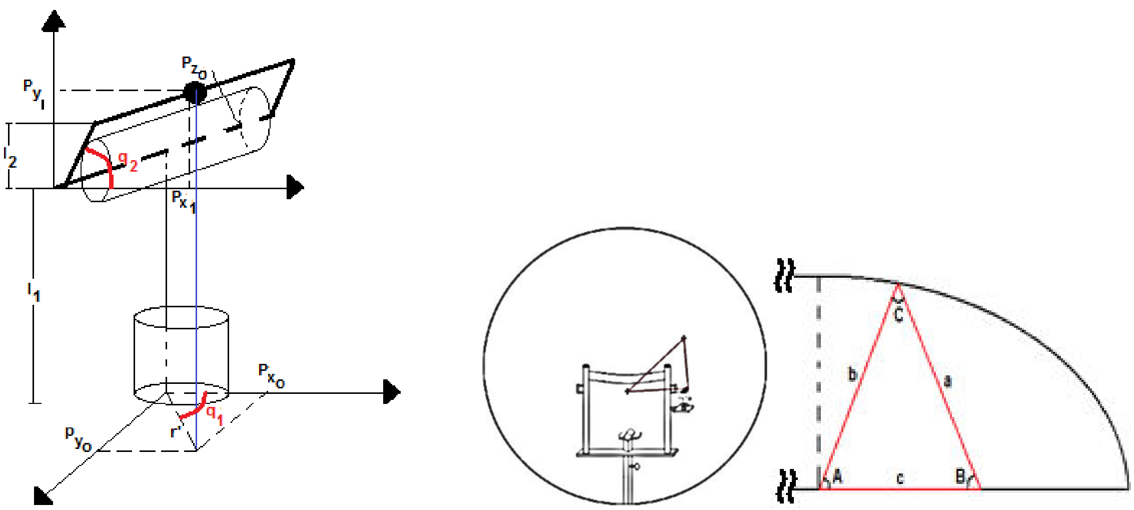

(a) (b)

Figure 2. (a) Representation of laser servo-driver for inverse kinematics analysis; (b) Representation of the lag angle, B, of the internal servomechanism (magnified version of the chin-rest).

3. Control Mechanisms of the Device

3.1. Therapy Design Software

The Therapy Designer Software is the most important part in the control mechanism of the proposed device and the light sequences (therapy) can be handled with the software process we describe here. After a preliminary medical visual field examination, the ophthalmologists must design a special visual therapy for each patient depending upon the diagnosis.

The therapies are divided in two main groups: middle-long distance therapies and short distance therapies. The short distance therapy is further divided into (a) complete visual field or (b) macular, see Figure 3 (Top). When a patient begins the treatment with the device he or she will have short distance therapies for the prescribed time suggested by the ophthalmologist.

Note that the complete visual field therapy stimulates different parts in the entire visual field whereas macular therapy stimulate only a small part of the visual field, only the first 10° of vision range. In contrast, middle-long distance therapies are not developed inside the device; instead the patient must sit watching a wall, where the stimuli will be presented. Figure 3 (Bottom) shows the sequence selectors for the three different cases. The therapist will choose a desired number of sequences according to the results of the examination to each patient; hence it is completely patient dependent.

Once the therapist finishes the particular design of the stimuli sequence, the software automatically displays a window where he can save the customized patient-specific details for future use as a text file.

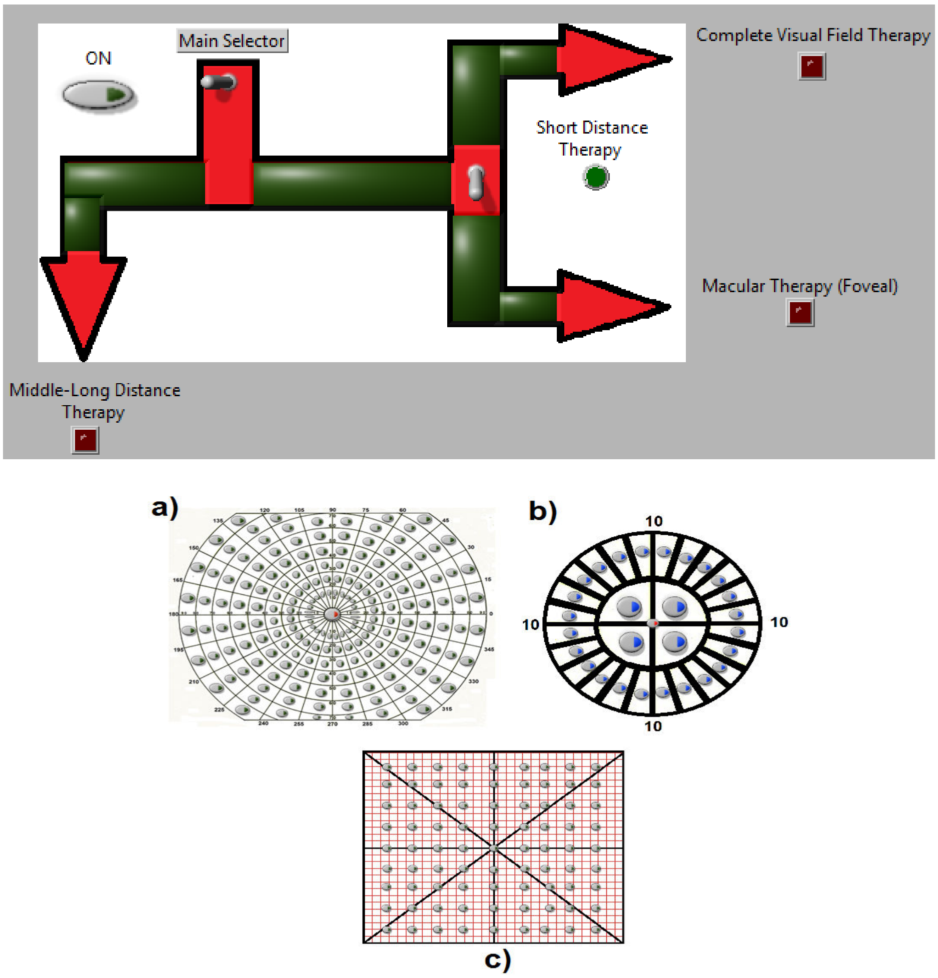

Figure 3. (Top): Illustration of the therapy selection main menu. This enables the user to select one of three options for the therapy. Stimuli sequence selectors; (Bottom): (a) Short distance – complete visual field; (b) Short distance – macular; (c) Middle-long distance.

3.2. Therapy Player Software

Figure 4(a) shows the display window of the therapy player software. Once the customized patient-specific text file has been created the control software reads it and sends signals to the microcontroller. Every number in the created file has an equivalent value in zenith and azimuth, and this conversion is encoded in an internal value table. When the program is running, first the therapist must select the stimuli time and the therapy time. Internally, the software selects it according the following equations:

$$t_t = \theta_{servo}\left(t_{spin} + t_{tol}\right) + t_{stimuli} \tag{6}$$

$$T = Nt_t \tag{7}$$

Where t_t time expended by the servomotors to point the laser to a given position and execute a laser beam sequence; t_{spin} is the time that a servomotor needs to spin one degree; t_{tol} is a given the tolerance time; θ_{servo} is the addition of degrees that both servos in a laser driver need to spin point the laser in a given position; $t_{stimuli}$ is the time expended in execute a laser beam, between 250 and 605 ms (Weiskrantz *et al*., 1991); T is the total time of all repetitions in a therapy, suggested between 20 and 60 minutes and N is the number of repetitions in a therapy.

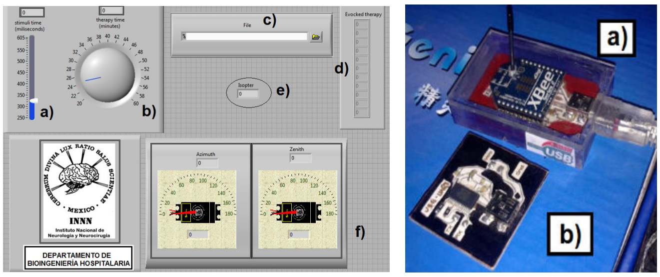

(a) (b)

Figure 4. (a) Therapy player software screen, where a) is the stimuli time, b) is the total therapy time, c) is the file path, d) displays the numeric values of each sequence of the therapy, e) shows the current value, and f) shows the current lag angle for zenith and azimuth values; (b) USB mechanism for conversion, where a) USB-UART converter, and b) USB-Zigbee converter.

When all the time parameters are selected, the next step is to select the desired text file. Then all the values of the list are displayed and the execution starts automatically. There is also a numeric indicator to see the current value in execution. Zenith and azimuth values of the laser beam are converted from the value table to a lag angle value using (4). The values are displayed in a modified-numeric indicator that appears like a servomotor. Each the lag angle value is converted into the hexadecimal format and then converted into a serial format to be sent to the microcontroller via USB.

3.3. Communication Between the Therapy Player Software and the Microcontroller

Modern computers rarely have RS232 inputs, because USB ports had gradually substituted it. USB protocol is completely different than RS232 neither in age nor in voltages and transfer rate, that is why it is necessary to use an interface to connect a single 8-bit microcontrller's UART to USB port. The FT232RL is a TSSOP28 package integrated circuit manufactured by FTDI®, it is an USB-UART is a USB controller that can each appear as a virtual COM port on a USB host. Each chip has a full-speed USB device port. The FT232RL converts between USB and an asynchronous serial interface.

Sometimes health centers do not have much storage space to store the complete device as the proposed one here, and hence it is better to consider the use of wireless technology for data storage and transmission. Further, this enhances the isolation of external distractors for the patients who undergo the therapies.

For this purpose, we consider XBee modules, which are wireless transceivers manufactured by Maxstream®, they utilize the IEEE 802.15.4 protocol (commonly known as Zigbee protocol). This protocol known as a Low-Rate, Wireless Personal Area Network (LR-WPAN) provides up to 250 kbps of data through put between nodes on a network. Note that both, FT232RL-based circuits and XBee modules are directly compatible, because the integrated circuit has a 3.3V output, what can be used as voltage source for the XBee (see Figure 4(b)).

The instructions are sent via USB and converted into serial format and then to Zigbee format. Zigbee wireless signal is received and converted into serial format again and a microcontroller receives the respective instructions to control by PWM the servomotors, and with digital pulses the lasers and buzzers. Thus, the proposed servo-motorized laser devise and the software module described here can be seamlessly integrated into existing ophthalmological tools and operational systems. Moreover, the wireless transmission makes it possible to be cost effective without sacrificing the data transmission rates and storage capacity.

4. Conclusion

In this paper we outlined a novel servo-motorized laser device and associated software control mechanism that is used in visual pathways diseases therapies. We believe this device is a good option to enhance visual abilities for patients with known hemianopia, quadrantanopia, scotoma and other types of cortical damages. Recent studies using the PET and fMRI imaging and detailed examinations suggest neuroplasticity effects due to learning in occipital region (Henriksson *et al.*, 2007; Pascual-Leone *et al.*, 2011). Currently we are adapting this devise and the corresponding control mechanism for various visual pathways diseases therapies. Further, extensive patient specific and multi-center examinations, validations, and data processing define our future work.

5. Conflicts of Interest

The authors declare no conflict of interest.

References

Garoutte, B., (1981), Survey of functional neuroanatomy (1st edition). Greenbrae CA: Jones Medical Publications.

Lane, A. R., Smith, D. T., Schenk, T. (2008). Clinical treatment options for patients with homonymous visual field defects. Clinical ophthalmology, 2, 93-102.

Schreiber, A., Vonthein, R, Reinhard, J. Trauzettel-Klosinski, S., Connert, C., Schiefer, U. (2006). Effect of visual restitution training on absolute homonymus scotomas. Neurology, 67, 143-145.

Koons, P., Scott, J., Kingston, J., Goodrich, G. L. (2010). Scanning training in neurological visual loss: case studies. Eye and Brain, 2, 47-55.

Weiskrantz, L., Harlow, A., Barbur, J. L. (1991). Factors affecting visual sensitivity in a hemianopic subject. Brain, 114, 2269-2282.

Romano, J. G. (2009). Progress in rehabilitation of hemianopic visual field defects. Cerebrovascular Diseases, 27 (suppl 1), 187-190.

Marshall, R. S., Ferrera, J. J., Barnes, A., Zhang, X., O'Brien K. A., Chmayssani, M., Hirsch, J., Lazar, R. M. (2008). Brain activity associated with simulation therapy of the visual borderzone in hemianopic stroke patients. Neurorehabilitation and Neural Repair, 22, 136-144.

Henriksson, L., Raninen, A., Näsänen, R., Ryvärinen, L., Vanni, S. (2007). Training-induced cortical representation of a hemianopic hemifield. Journal of Neurology, Neurosurgery & Psychiatry, 78, 74-81.

Pascual-Leone, A., Freitas, C., Oberman, L., Horvath, J. C., Halko, M., Eldaief, M., Bashir, S., Vernet, M., Shafi, M., Westover, B., Vahabzadeh-Hagh, A. M., Rotenberg, A. (2011). Characterizing brain cortical plasticity and network dynamics across the age-span in health and disease with TMS-EEG and TMS-fMRI. Brain Topography, 24, 302-315.

Borah, J. (2006). Measurement techniques for eye movement. Encyclopedia of Medical Devices and Instrumentation, 3, 263-286.

Halswanter, T. (1995). Mathematics of three-dimensional eye rotations. Vision Res, 12, 1727-1739.

Pambakian, A. L. M., Woodings, D. S., Patel, N., Morland, A. B., Kennard, C., Mannan, S. K. (2000). Scanning the visual world: a study of patients with homonymous hemianopia. Journal of Neurology, Neurosurgery & Psychiatry, 69, 751-759.

Panero, J., Zelnik, M. (1996). Las dimensiones humanas en los espacios interiores (7th ed). Valle de Bravo, México: Ediciones G. Gili. Original title: Human dimension and interior space, New York: Watson-Guptill Publ. Retrieved from http://179.33.0.50/~colfps/pkaz/libros/diseno/las-dimensiones-humanas.pdf

Fu, K. S., González, R. C., Lee, C. S. G. (1987). Robotics: Control, sensing, vision and intelligence (1st edition). New York, NY: McGraw-Hill.

Spong, M. W., Hutchinson, S., Vidyasagar, M. (2005). Robot modeling and control. New York: John Wiley and Sons Inc.